

## IT-SOFC Based on a Disaggregated Electrospun LSCF Nanofiber Electrode Deposited onto a GDC Electrolyte Disc: Preparation Technique and Morphological Characterization

C. Sanna<sup>1</sup>, A. Lagazzo<sup>1</sup>, E. M. Sala<sup>2</sup>, R. Botter<sup>1</sup>, P. Costamagna<sup>3,†</sup>

<sup>1</sup> Department of Civil, Chemical and Environmental Engineering (DICCA), University of Genoa, Italy

<sup>2</sup> Department of Energy Conversion and Storage, Technical University of Denmark, Frederiksborgvej 399, DK-4000 Roskilde, Denmark

<sup>3</sup> Department of Chemistry and Industrial Chemistry (DCCI), University of Genoa, Italy

Received May 15, 2018    Revised July 12, 2018

Laboratory-size intermediate temperature solid oxide fuel cells (IT-SOFCs) are manufactured, based on  $\text{La}_{0.6}\text{Sr}_{0.4}\text{Co}_{0.2}\text{Fe}_{0.8}\text{O}_{3-\delta}$  (LSCF) nanofiber electrodes applied onto  $\text{Ce}_{0.9}\text{Gd}_{0.1}\text{O}_{1.95}$  (GDC) electrolyte discs. The LSCF nanofiber electrodes are produced through electrospinning. The electrospun tissue is gently disaggregated in  $\alpha$ -terpinol before being applied onto the electrolyte, in order to break the fibers into segments, while preserving their morphology. GDC electrolytes are obtained by uniaxial pressing of the GDC powders, followed by sintering. The dispersed nanofibers are deposited onto the electrolyte to form symmetrical IT-SOFCs, which are then heat treated. SEM characterisation of the heat treated IT-SOFCs proves that the nanofibers morphology is preserved, forming a 3-D structure with many contact points among the fibers themselves, which is expected to feature simultaneously enhanced charge conduction and electrochemical reaction. The cells are ready for electrochemical impedance spectroscopy (EIS), which is the ideal tool to characterize the electrochemical performance of the disaggregated electrospun LSCF nanofiber electrodes.

**Key words:** nanofiber; electrospinning; intermediate temperature solid oxide fuel cell (IT-SOFC);  $\text{La}_{0.6}\text{Sr}_{0.4}\text{Co}_{0.2}\text{Fe}_{0.8}\text{O}_{3-\delta}$  (LSCF); sol-gel synthesis;  $\text{Ce}_{0.9}\text{Gd}_{0.1}\text{O}_{1.95}$  (GDC).

### INTRODUCTION

The upward trend of global energy emissions, and their likely multiple adverse effects, compel the adoption of eco-innovative energy supply solutions, to foster world transition into a paradigm of sustainability [1]. Fuel cells, featuring high efficiency and environmental compatibility, are considered the preferable candidate to substitute the conventional energy conversion technologies. Solid oxide fuel cells (SOFCs), based on ceramic materials, offer several advantages over other types of fuel cells, mainly due to the use of non-noble metals as catalyst, the possibility of being moulded in a variety of shapes, and the high fuel flexibility, which allows 100% tolerability towards CO and around 5% tolerability towards  $\text{CH}_4$  (depending on the SOFC operating temperature) [2]. On the one hand, the traditionally high SOFC operating temperature (around  $900^\circ\text{C}$ ) matches perfectly the feeding temperature of gas turbines (GTs), allowing an ideal coupling in hybrid cycles featuring up to 65% efficiency. Unluckily, on the other hand, this

high operating temperature involves technological problems, primarily due to the different thermal expansion coefficient (TEC) of the SOFC components, causing delamination and eventually breaking. Another problem is that the high operating temperature favours an almost instantaneous development of the steam reforming of  $\text{CH}_4$ , whose endothermic behaviour can cause a steep temperature drop dangerous for the mechanical stability of the ceramic materials, limiting to about 5% the amount of  $\text{CH}_4$  which can be fed directly into the SOFC and making internal  $\text{CH}_4$  steam reforming practically unfeasible. These problems are heavily mitigated by lowering the operating temperature down to  $550\text{--}850^\circ\text{C}$  [3,4], which is the so-called intermediate temperature range. Furthermore, lower temperatures are expected to mitigate degradation, reduce sealing problems, enable the use of less expensive materials in the balance of plant and finally improve the response to rapid start-up. However, lowering the operating temperature also lowers the SOFC performance, since electrodes and electrolyte materials become less conductive. Furthermore, the kinetics of the electrochemical reactions decreases exponentially as temperature decreases; indeed, the

---

To whom all correspondence should be sent:  
E-mail: paola.costamagna@unige.it

poor activity of the cathode is one of the key obstacles for the development of IT-SOFCs [5]. For these reasons, innovative materials are under investigation. For the electrolyte,  $\text{Ce}_{0.9}\text{Gd}_{0.1}\text{O}_{1.95}$  (GDC) is used [6], while  $\text{La}_{0.6}\text{Sr}_{0.4}\text{Co}_{0.2}\text{Fe}_{0.8}\text{O}_{3-\delta}$  (LSCF), which is a well-known MIEC (mixed ionic electronic conductor), is considered as one of the most promising cathodes [3]. The number of active sites for the oxygen reduction reaction (ORR) is expected to increase dramatically with the increase of the specific surface area [7,8], and thus new electrode morphologies and architectures are under development. In this framework, nano-structured electrode scaffolds, often obtained through the electrospinning technique, are intensively investigated [9]. This preparation method offers advantages in terms of simplicity, efficiency, low cost and high degree of reproducibility of the obtained materials [10]. In addition, it allows to manufacture complex nanostructures, usually fiber-made, with specific properties, such as high surface area, high porosity and excellent mechanical strength, which make them very suitable for IT-SOFC electrode applications [11,2].

In the present paper, we present an innovative preparation technique for symmetrical cells employing LSCF electrospun electrodes, applied symmetrically onto GDC electrolyte discs. The LSCF tissue manufactured through the electrospinning technique is gently disaggregated before being applied onto the GDC electrolyte, in order to obtain short fiber segments which form a 3-D structure with a high number of contact points between the fibers, to be tested through the electrochemical impedance spectroscopy (EIS) technique in order to assess the electrochemical performance.

## EXPERIMENTAL

### Materials

LSCF fibers are synthesized using nitrates as precursors: lanthanum (III) nitrate hexahydrate  $\text{LaN}_3\text{O}_9 \cdot 6\text{H}_2\text{O}$ , strontium nitrate  $\text{Sr}(\text{NO}_3)_2$ , cobalt nitrate hexahydrate  $\text{Co}(\text{NO}_3)_2 \cdot 6\text{H}_2\text{O}$  and iron (III) nitrate  $\text{Fe}(\text{NO}_3)_3 \cdot 9\text{H}_2\text{O}$ . Ethanol, N,N-Dimethylformamide (DMF) and distilled water are used as solvents. Polyvinylpyrrolidone (PVP) is

used as carrier polymer. All these materials are provided by Sigma-Aldrich.

LSCF granular electrodes are manufactured using  $\text{La}_{0.6}\text{Sr}_{0.4}\text{Co}_{0.2}\text{Fe}_{0.8}\text{O}_{3-\delta}$  powders provided by Sigma-Aldrich (product code 704288, particle size 0.7 - 1.1  $\mu\text{m}$ , surface area 5-8  $\text{m}^2/\text{g}$ ).

GDC powders used for the electrolyte preparation are supplied by Fuelcellmaterials (GDC10-TC powder, particle size 0.1-0.4  $\mu\text{m}$ , surface area 5.9  $\text{m}^2/\text{g}$ ). In the cases where the GDC powders are mixed with additives, 10 wt% ammonium polyacrylate/water and 5% polyvinyl alcohol (PVA)/water solutions are used, both supplied by Sigma-Aldrich.

### Preparation Procedures

#### LSCF nanofiber electrodes

LSCF fibrous electrodes are manufactured through electrospinning. The starting solution is prepared by dissolution of 0.178 g of  $\text{Sr}(\text{NO}_3)_2$  in 0.4 ml of distilled water. Subsequently, 4 ml of DMF and 6 ml of ethanol are added, followed by mixing for 2 minutes with magnetic stirrer. Then, 0.545 g of  $\text{LaN}_3\text{O}_9 \cdot 6\text{H}_2\text{O}$ , 0.122 g of  $\text{Co}(\text{NO}_3)_2 \cdot 6\text{H}_2\text{O}$  and 0.679 g of  $\text{Fe}(\text{NO}_3)_3 \cdot 9\text{H}_2\text{O}$  are added to the solution, followed by mixing for 10 minutes. Lastly, 1.24 g of PVP are added, followed by 24 h mixing (always with magnetic stirrer). With this procedure, the molar ratio of the elements La, Sr, Co, Fe in solution is 6:4:2:8 respectively. After preparation, the solution is fed into a single-needle electrospinning device (Spinbow), consisting of four main parts: high-voltage generator, volumetric pump (KD Scientific), syringe and cylindrical collector (diameter 4 mm), which turns and shifts in order to ensure homogenous thickness to the electrospun tissue. The operating parameters for the electrospinning device have been discussed in a previous paper [3], and are reported in Table 1.

The LSCF nanofibers are heat treated following the procedure reported below [3]:

- 1°C/min from 20°C to 350°C;
- 0.2°C/min from 350°C to 500°C;
- 1°C/min from 500°C to 800°C;
- 1°C/min from 800°C to 20°C.

**Table 1.** Operating parameters of the electrospinning device [3].

Flow rate [ml/h]	Voltage [kV]	Needle-Collector Distance [cm]	Collector Translation Speed [mm/s]	Collector Rotation Speed [rpm]
0.5	17	12	1000	750

### GDC electrolyte

For the preparation of the GDC electrolyte discs, two different ways of treating the raw GDC powders are employed. The first method consists in mixing a mass of 2 g of GDC powders with 50 mL of distilled water. Then 0.269 g of 10 wt% ammonium polyacrylate/water solution (dispersant) and 0.538 g of 10 wt% PVA/water solution (binder), and finally 50 mL distilled water are added, followed by 12 h treatment in an ultrasonic device (sonicator UR1 Retsch ultrasonic bath). Once the solution is dried, it is sieved and then it is ready for pressing. In the second procedure, the raw GDC powders are pressed with no preliminary treatment. Uniaxial pressing is performed, which is selected since it allows minimisation of the void degree of the electrolyte pellet. The press die body (13 mm diameter), is filled from the bottom: in this way the GDC powder distribution has a high degree of uniformity, resulting in a low void degree of the final electrolyte pellet. Applied pressure ranges from 50 MPa to 100 MPa. The GDC discs are then sintered in a furnace, following the procedure reported below:

- 1°C/min from 20°C to 200°C;
- 0.1°C/min from 200°C to 300°C;
- 10°C/min from 300°C to  $T_{max}$ ;
- $T_{max}$  for 4h;
- 1°C/min from  $T_{max}$  to 20°C.

Three different values of  $T_{max}$  are tested: 1350°C, 1420°C and 1580°C. In all cases, after sintering, the GDC electrolyte diameter is 1.1 cm.

### Symmetrical cell assembly

The LSCF nanofiber tissue is gently disaggregated in  $\alpha$ -terpinol in the sonicator for 8 seconds. The resulting mixture is deposited symmetrically onto both faces of the GDC electrolyte discs.

Furthermore, symmetrical cells with LSCF granular electrodes are manufactured as well. In this case, the LSCF powder is dispersed in  $\alpha$ -terpinol and deposited symmetrically onto the GDC electrolyte. All the symmetrical cells are heat treated following the procedure reported below:

- 1°C/min from 20°C to 350°C;
- 0.2°C/min from 350°C to 500°C;
- 1°C/min from 500°C to 1000°C;
- 1°C/min from 1000°C to 20°C.

In all cases, after heat treatment the electrodes have diameter 0.9 cm and thickness about 40  $\mu$ m.

### Characterisation methodology

With all the samples presented in this work, micrograph characterizations are carried out through a scanning electron microscope (SEM)

Hitachi S-2500. SEM images of the GDC electrolyte surface are used to evaluate the average superficial porosity through the intercept method, using a 0.32  $\mu$ m grid.

In addition, electrolytes are characterized in terms of geometrical density, Archimedes' principle density, mechanical bending, and thermal etching. Geometrical density is evaluated by measuring the pellet through a micrometer. The mechanical bending test is used to determine the Young's modulus and the ultimate strength point. The test is carried out through a Zwick-Roell Z0.5 instrumentation. The electrolyte disc is placed on an o-ring and a force is impressed through a sphere positioned in the centre (Fig.1). The ultimate strength (P) is measured at the breaking point of the sample, while the Young's modulus (E) and the maximum stress ( $\sigma_{max}$ ) are calculated as follows [12]:

$$\sigma_{max} = \frac{6P}{4\pi t^2} \left( (1 + \nu) \ln \left( \frac{r}{e'} \right) + 1 \right) \quad (1)$$

$$e' = (\sqrt{1.6e^2 + t^2}) - 0.675t \quad (2)$$

$$E = \frac{0.552Pr^2}{t^3 y_m} \quad (3)$$

where  $\sigma_{max}$  [Pa];  $\nu$  = Poisson ratio – (assumed as 0.3);  $e$  = support footprint – (assumed as 0) [m];  $P$  = ultimate strength [N];  $r$  = o-ring radius [m];  $t$  = sample thickness [m];  $y_m$  = deformation [m];  $E$  = Young's modulus [Pa].

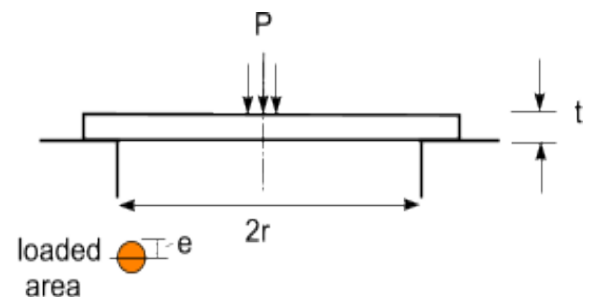


**Fig.1.** Schematic representation of the mechanical bending test.

GDC pellets are thermally etched, and then the linear intercept method is applied to the SEM pictures to evaluate the grain size [13]. The linear intercept method consists in drawing a set of randomly positioned line segments on the micrograph, counting the number of times each line segment intersects a grain boundary, and finding the ratio of intercepts to line length.

## RESULTS AND DISCUSSION

*LSCF nanofibers*

SEM pictures of the heat treated LSCF nanofibers are reported in Fig. 2. In agreement with the results previously reported in [3], the nanofibers are continuous and randomly arranged. The average diameter is around 250 nm.

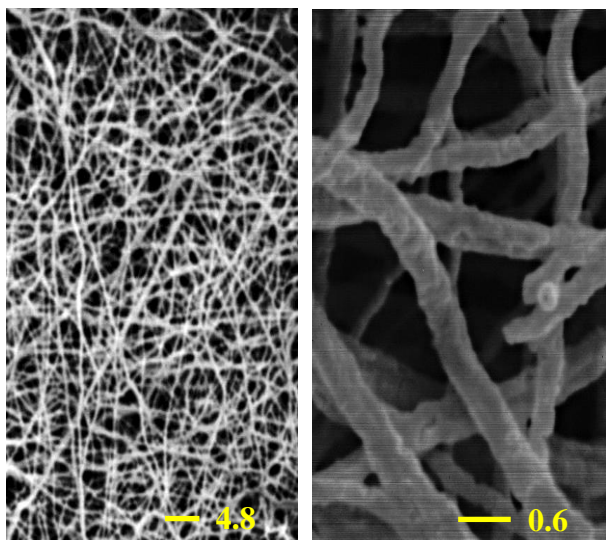


**Fig. 2.** SEM pictures of heat treated LSCF nanofibers.

*GDC electrolyte*

Fig. 3 reports SEM pictures of the surface of three different GDC discs. All the discs are obtained by mixing the GDC powders with a dispersant and a binder (first preparation method), followed by pressing at 80 MPa. Then, the GDC discs are sintered using three different  $T_{\max}$  (1350°C, 1420 °C or 1580 °C). Fig.3(a) shows that with  $T_{\max} = 1350^{\circ}\text{C}$ , a high residual porosity (void degree) is clearly visible. Fig.3(b) displays that increasing the sintering temperature up to  $T_{\max} = 1420^{\circ}\text{C}$ , the residual porosity is significantly decreased. Finally, a further increase of sintering temperature up to  $T_{\max} = 1580^{\circ}\text{C}$ , leads to a further reduction of the residual porosity, as shown in Fig.3(c).

Fig. 3 shows that the reduction of residual porosity observed with increasing the sintering temperature. In particular, Fig. 3 (a) displays an intermediate stage of sintering, with interconnected porosity, while Fig. 3 (b) and (c) display a final stage of sintering with isolated pores. The increased stage of sintering is accompanied by an enlargement of grain size. This is an important parameter since it affects significantly the oxygen ion conductivity of the GDC electrolyte, as demonstrated by [14,15].

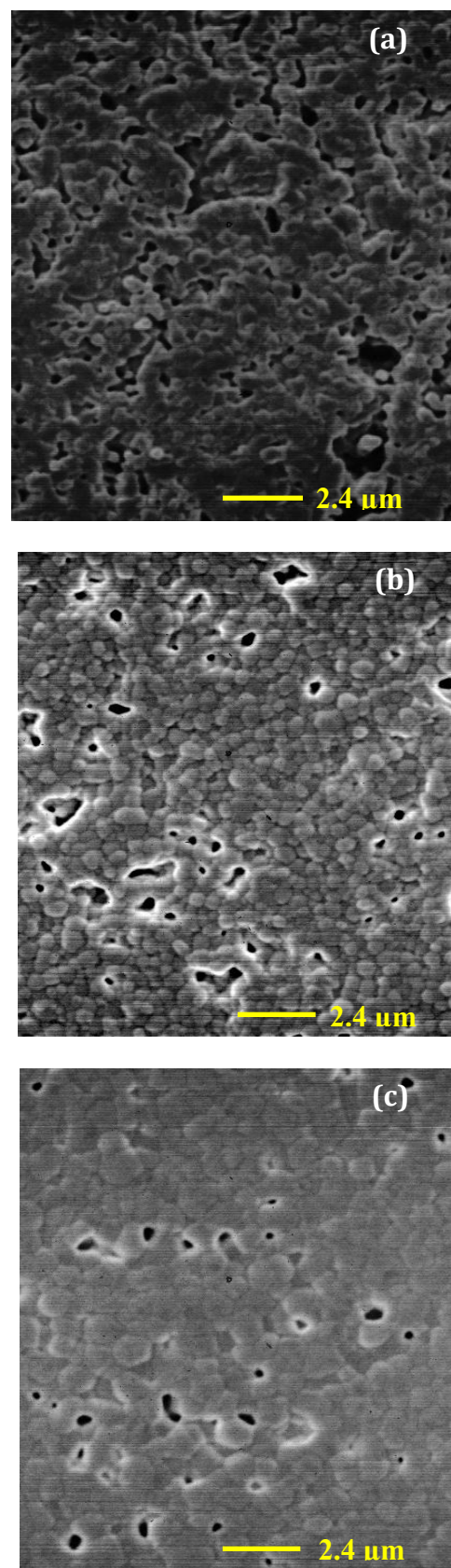


**Fig. 3.** SEM image of the surface of GDC electrolyte discs obtained by uniaxial pressing at 80 MPa, after sintering at  $T_{\max}$  (a) 1350 °C, (b) 1420 °C, and (c) 1580 °C.

Nevertheless, Fig. 3 (c) shows that some residual porosity is clearly visible even with the

highest sintering temperature of 1580°C. This suggests that the dispersant and the binder added to the raw GDC powders may interfere with the process of grain agglomeration and growth during sintering. Thus, a different procedure is experimented, where the raw GDC powders are not pre-treated, but instead they are pressed straight as-received (second preparation method). Keeping the maximum sintering temperature fixed at 1580°C, the uniaxial pressing process is investigated by applying a pressure of 50 MPa or 100 MPa. Fig.4 shows SEM images of the surface of the GDC discs, displaying a reduced porosity and an increased grain size, especially with the highest

applied pressure of 100 MPa. Tab. 2, for completeness, reports geometrical and Archimedes' density measurements. Considering that the bulk GDC density is 7.2 g/cm<sup>3</sup>, for the sample pressed at 100 MPa the relative density is 0.924 according to the geometrical density measurement, and 0.937 according to the Archimedes' density measurement

The average superficial porosity, calculated with the intercept method applied to Fig. , is 0.1% for the electrolyte pressed at 50 MPa, whereas it is 0.04% for the electrolyte pressed at 100 MPa, which is in agreement with the results obtained from the density characterisation.

**Table 2.** Features of GDC electrolyte discs obtained with different applied pressures.

GDC disc						
Applied pressure [MPa]	Weight [g]	Diameter [cm]	Thickness [cm]	Volume [cm <sup>3</sup> ]	Geometrical Density [g/cm <sup>3</sup> ]	Archimedes' Density [g/cm <sup>3</sup> ]
50	0.224	1.108	0.037	0.036	6.299	6.503
100	0.202	1.110	0.032	0.031	6.651	6.743

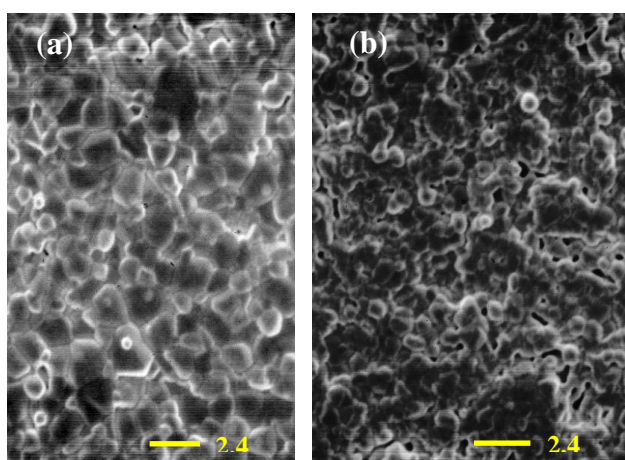


**Fig. 4.** SEM images of the surface of GDC electrolyte discs obtained by uniaxial pressing at (a) 50 MPa, and (b) 100 MPa.

An SEM picture of the surface of the GDC disc pressed at 100 MPa, after thermal etching, is reported in Fig. 5. The grain size evaluated through the linear intercept method is 0.5 μm.

The GDC disc obtained through uniaxial pressing at 100 MPa is further characterized through mechanical tests. The stress and strain diagram is reported, the corresponding ultimate strength is  $P = 11.7$  N, the Young's modulus is  $E = 0.12$  GPa, and the maximum stress is  $\sigma_{max} =$

30.5 MPa. All these features comply with the requirements for a GDC disc to be used as the electrolyte of an IT-SOFC. Thus, the samples obtained by pressing the as-received GDC powders at 100 MPa, followed by sintering at  $T_{max} = 1580^\circ\text{C}$ , are selected for manufacturing the symmetrical cells.

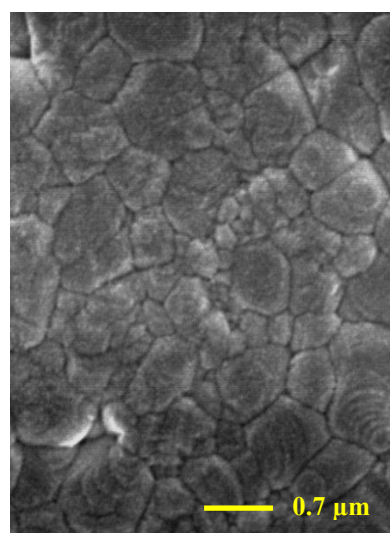


**Fig. 5.** SEM image of the surface of a GDC electrolyte disc obtained by uniaxial pressing at 100 MPa, after thermal etching.

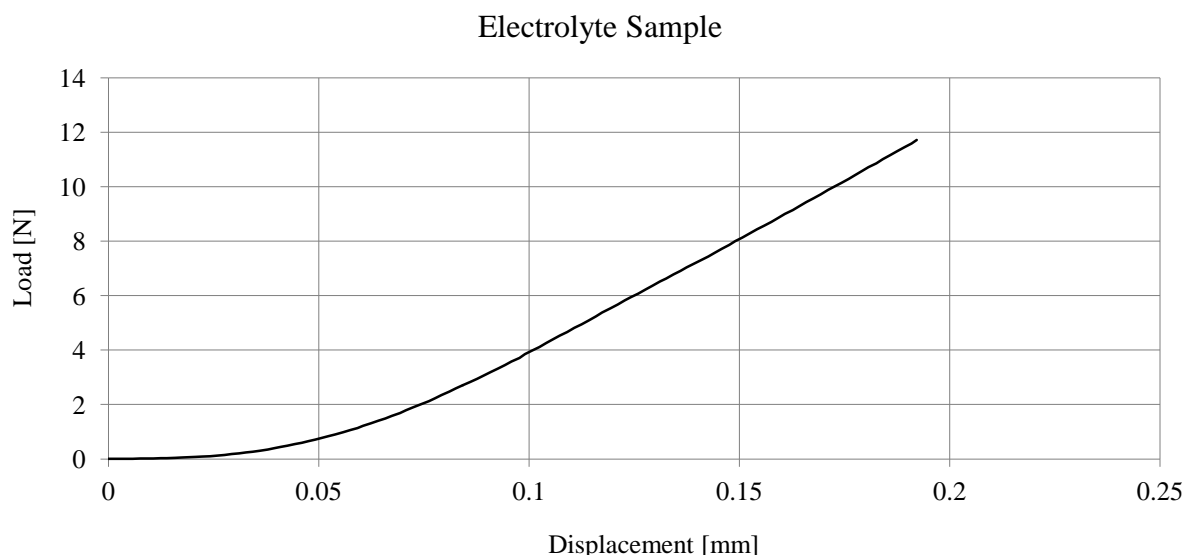


**Fig.6.** Experimental load and displacement diagram of the GDC electrolyte disc obtained by uniaxial pressing at 100 MPa, followed by sintering at  $T_{\max} = 1580^{\circ}\text{C}$ .

### Symmetrical cells

Symmetrical cells are prepared employing LSCF nanofibers or LSCF granular powders, which are coupled to the GDC electrolyte. SEM pictures of the symmetrical cells (top-view) are reported in Fig.7, clearly displaying the electrodes. Fig. 7(a) and (b) show that the morphology of the fibers is preserved after disaggregation, even if the fibers are clearly broken into segments. This 3-D structure with many contact points between the fibers, is

expected to feature simultaneously enhanced charge conduction and electrochemical reaction [3]. The high void degree is ideal to accommodate, in future developments, a high degree of infiltrations, which are expected to improve the electrochemical performance [3]. Fig.7(c) shows the morphology of the LSCF granular electrode, clearly displaying that the LSCF particles have irregular shape. In this case the void degree is much lower than with the fibrous electrode.

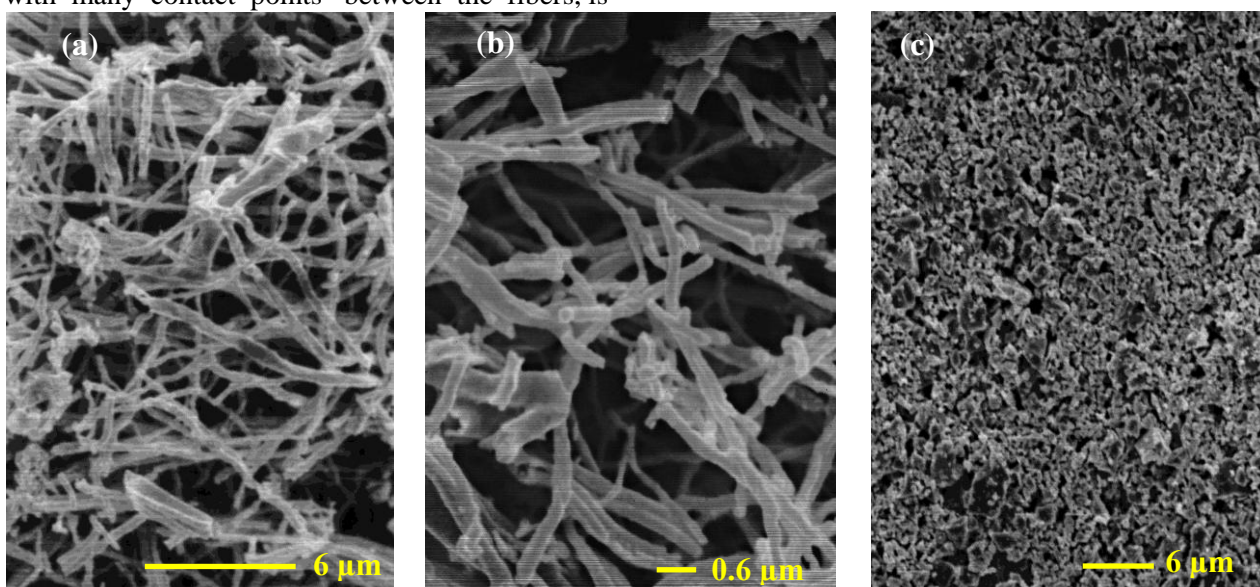


**Fig.7.** SEM pictures of LSCF electrodes (top view) after application onto GDC discs: (a) and (b) nanofiber electrode, and (c) granular electrode.

## CONCLUSIONS

Laboratory symmetrical IT-SOFCs of 1.1 cm of diameter (electrode diameter 0.9 cm) are developed, employing in-house manufactured electrospun LSCF fibrous electrodes deposited onto in-house developed GDC electrolyte discs. In the electrodes, the fibers do not form a unique continuous wire along the whole electrode, but rather they are gently disaggregated to form a network of randomly distributed segments. As a comparison, symmetrical laboratory cells employing granular LSCF electrodes deposited on the same type of GDC electrolytes are manufactured as well.

Future plans include (i) testing through EIS, in order to assess the electrochemical performance; and (ii) comparison with laboratory IT-SOFCs employing LSCF electrospun electrodes applied onto the GDC electrolyte with a different procedure [16], where the fibers form a unique continuous wire along the whole electrode.

## REFERENCES

1. A. Mehmeti, S.J. McPhail, D. Pumiglia, M. Carlini, *J. Power Sources*, **325**, 772, (2016).
2. S.T. Aruna, L.S. Balaji, S. S. Kumar, B. Shri Prakash, *Renew. Sust. Energ. Rev.*, **67**, 673, (2017).
3. A. Enrico, B. Aliakbarian, A. Lagazzo, A. Donazzi, R. Botter, P. Perego, P. Costamagna, *Fuel Cells*, **17**, 415 (2016).
4. Ding D., Li X., Lai S. Y., Gerdes K. and Liu M., *Energy Environ. Sci.*, **552** (2014).
5. J. Cheng, Y. Jun, J. Qin, S.H. Lee, *Biomaterials*, **114**, 121 (2017).
6. J.M. Ralph, A.C. Schoeler, M. Krumpelt, *J. Mater. Sci.*, **36**, 1161 (2001).
7. E. Zhao, Z. Jia, X. Liu, K. Gao, H. Huo, Y. Xiong, *Ceram. Int.*, **40**, 14891 (2014).
8. L.M. Acuña, J. Peña-Martínez, D. Marrero-López, R.O. Fuentes, P. Nuñez, D.G. Lama, *J. Power Sources*, **196**, 9276 (2011).
9. A. Enrico, P. Costamagna, *J. Power Sources*, **272**, 1106 (2014).
10. J.T. Sill, H.A. von Recum, *Biomaterials*, **29**, 1989 (2008).
11. S. Thenmozhi, N. Dharmaraj, K. Kadirvelu, H.Y. Kim, *Mater. Sci. Eng. B-Adv. Funct. Solid-State Mater.*, **217**, 36 (2017).
12. W.C. Young, R.G. Budynas, Roark's Formulas for Stress and Strain, McGraw-Hill Professional 8<sup>th</sup> Ed. (2011).
13. J.C. Russ, R.T. Dehoff, Practical Stereology, Springer 2<sup>nd</sup> Ed. (2000).
14. Y. Lin, S. Fang, D. Su, K.S. Brinkman, F. Chen, *Nat. Commun.*, **6**, 6824 (2015).
15. H. Bi, X. Liu, L. Zhu, J. Sun, S. Yu, H. Yu, L. Pei, *Int. J. Hydrog. Energy*, **42**, 11735 (2017).
16. A. Enrico, W. Zhang, M. Lund Traulsen, E.M. Sala, P. Costamagna, P. Holtappels, *J. Eur. Ceram. Soc.*, **38**, 2677 (2018).

СТ-ТОКГ на базата на дисегрегирани електроизплетени от нановлакна LSCF електроди, нанесени върху GDC електролит: начин на изработка и морфологична характеристика

К. Санна<sup>1</sup>, А. Лагацо<sup>1</sup>, Е.М. Сала<sup>2</sup>, Р. Ботер<sup>2</sup>, П. Костамања<sup>3, †</sup>

<sup>1</sup> Катедра по гражданско, химическо и екологично инженерство (DICCA), Университет в Генуа, Италия

<sup>2</sup> Министерство на енергийната конверсия и съхранение, Технически университет на Дания, Фредериксборгей 399, DK-4000 Рокишилд, Дания

<sup>3</sup> Катедра по химия и индустриална химия, Университет в Генуа, Италия

Постъпила на 15 май 2018г.; приета на 12 юли 2018г.

(Резюме)

Разработени са средно температурни твърдо оксидни горивни клетки (СТ-ТОКГ), на базата на електроди от  $\text{La}_{0.6}\text{Sr}_{0.4}\text{Co}_{0.2}\text{Fe}_{0.8}\text{O}_{3-\delta}$  (LSCF) нановлакна, нанесени върху  $\text{Ce}_{0.9}\text{Gd}_{0.1}\text{O}_{1.95}$  (GDC) електролит. Електродите от LSCF нановлакна се получават чрез електроизплетане. Електроизплетената тъкан се дисегрегирани в  $\alpha$ -терпинол, преди да се нанесе върху електролита, с цел да се накъсат влакната на отделни сегменти, като се запази тяхната морфология. Електролитите GDC се получават чрез еднократно пресоване на GDC прахове, последвано от синтероване. Диспергираните нановлакна се отлагат върху електролита, за да образуват симетрични клетки, които след това се загряват. Характеризацията със СЕМ на топлинно обработените ИТ-ТОКГ образци доказва, че се запазва морфологията на нановлакните влакна, образувайки 3-D структура с много контактни точки между самите влакна, което се очаква да се характеризира едновременно с подобрени проводимост и електрохимична реактивност. Клетките са изследвани с електрохимична импедансна спектроскопия (ЕИС), която е идеалният инструмент за характеризиране на електрохимичните експлоатационни качества на дисегрегирани електроизплетени от нановлакна LSCF електроди.